

## Intercomparison of Satellite Retrieved Aerosol Optical Depth over the Ocean

GUNNAR MYHRE,<sup>\*,+</sup> FRODE STORDAL,<sup>\*,+</sup> MONA JOHNSRUD,<sup>\*</sup> ALEXANDER IGNATOV,<sup>#</sup>  
MICHAEL I. MISHCHENKO,<sup>@</sup> IGOR V. GEOGDZHAYEV,<sup>@</sup> DIDIER TANRÉ,<sup>&</sup> JEAN-LUC DEUZÉ,<sup>&</sup>  
PHILIPPE GOLOUB,<sup>&</sup> TERUYUKI NAKAJIMA,<sup>\*\*</sup> AKIKO HIGURASHI,<sup>++</sup> OMAR TORRES,<sup>##</sup>  
AND BRENT HOLBEN<sup>@@</sup>

<sup>\*</sup>Norwegian Institute for Air Research, Kjeller, Norway

<sup>+</sup>Department of Geophysics, University of Oslo, Oslo, Norway

<sup>#</sup>NOAA/NESDIS/Office of Research and Applications/Climate Research and Applications Division, Washington, D.C.

<sup>@</sup>NASA Goddard Institute for Space Studies, New York, New York

<sup>&</sup>Laboratoire d'Optique Atmosphérique, CNRS, U.S.T. de Lille, Villeneuve d'Ascq, France

<sup>\*\*</sup>Center for Climate System Research, University of Tokyo, Tokyo, Japan

<sup>++</sup>National Institute for Environmental Studies, Tsukuba, Japan

<sup>##</sup>Joint Center for Earth Systems Technology, University of Maryland, Baltimore County, Baltimore, Maryland

<sup>@@</sup>NASA Goddard Space Flight Center, Biospheric Sciences Branch, Greenbelt, Maryland

(Manuscript received 15 August 2002, in final form 29 November 2002)

### ABSTRACT

For an 8-month period aerosol optical depth (AOD) is compared, derived over global oceans with five different retrieval algorithms applied to four satellite instruments flown on board three satellite platforms. The Advanced Very High Resolution Radiometer (AVHRR) was flown on board *NOAA-14*, the Ocean Color and Temperature Scanner (OCTS) and the Polarization and Directionality of the Earth's Reflectances (POLDER) on board the *Advanced Earth Observing Satellite (ADEOS)*, and the Total Ozone Mapping Spectrometer (TOMS) on board the Earth Probe satellites. The aerosol data are presented on the same format and converted to the same wavelength in the comparison and can therefore be a useful tool in validation of global aerosol models, in particular models that can be driven with meteorological data for the November 1996 to June 1997 period studied here. Large uncertainties in the global mean AOD are found. There is at least a factor of 2 difference between the AOD from the retrievals. The largest uncertainties are found in the Southern Hemisphere, and the smallest differences mostly near the continents in the Northern Hemisphere. The largest relative differences are probably caused by differences in cloud screening.

### 1. Introduction

Haywood et al. (1999) showed by combining satellite observations and a model that the direct aerosol effect is substantial over ocean under clear-sky conditions. Several observational studies indicate a significant influence on the cloud microphysics from anthropogenic aerosols (Wetzel and Stowe 1999; Rosenfeld 2000; Kuang and Yung 2000; Nakajima et al. 2001). The radiative forcing for both the direct and the indirect aerosol effect is very uncertain (Houghton et al. 2001), and the estimates of radiative forcing are mainly based on models.

With the large temporal and spatial variability in aerosol composition and abundance, satellite retrieval has become a very useful tool for studying aerosol characteristics (Kaufman et al. 1997; King et al. 1999; Mish-

chenko et al. 2002) and comparing with models. There have been some initial studies with global models and several aerosol components included where comparison with satellite retrievals have been performed (Takemura et al. 2000; Penner et al. 2002; Chin et al. 2002). Such comparisons are very useful and similar studies will presumably be performed in the future.

Most of the past satellite aerosol retrievals are based on one or two channels (King et al. 1999) that lead to information on one or two aerosol properties: usually aerosol optical depth (AOD) and Ångström exponent for two-channel retrievals. A number of studies have demonstrated that aerosol retrievals from satellite are sensitive to two groups of factors: assumptions made in the retrieval algorithm (ocean reflectance, gaseous absorption, and aerosol microphysics), and quality of input satellite radiances used for aerosol retrievals (radiometric uncertainties and cloud contamination; e.g., Kaufman et al. 1990; Wagener et al. 1997; Ignatov et al. 1998; Kahn et al. 1998; Higurashi and Nakajima 1999; Mishchenko et al. 1999; Geogdzhayev et al. 2002; Ignatov 2002).

Corresponding author address: Dr. Gunnar Myhre, Department of Geophysics, University of Oslo, P.O. Box 1022, Blindern, Oslo 0315, Norway.  
E-mail: gunnar.myhre@geofysikk.uio.no

Over the last few years several pioneering investigations of aerosol characteristics have been performed (Husar et al. 1997; Nakajima and Higurashi 1998; Goloub et al. 1999; Mishchenko et al. 1999; Torres et al. 1998). These studies have used AOD (and some of them also Ångström exponent) derived over ocean for clear-sky conditions for different satellite instruments, such as the Advanced Very High Resolution Radiometer (AVHRR), the Ocean Color and Temperature Scanner (OCTS), the Total Ozone Mapping Spectrometer (TOMS), and the Polarization and Directionality of the Earth's Reflectances (POLDER). All the studies show distinct features for the aerosols on a global scale, including natural and human-influenced aerosols. A remaining task is to distinguish between natural and anthropogenic aerosols from the satellite retrievals (Boucher and Tanre 2000). Future satellite instruments will have larger capabilities in this respect (King et al. 1999).

Satellite retrievals over land have just become available for global conditions (Chu et al. 2002; Torres et al. 2002), and there has been one study of aerosol optical depth over Europe (Gonzalez et al. 2000). Other investigators have performed satellite retrievals over land using the aerosol index (Hsu et al. 1996; Herman et al. 1997; Deuze et al. 2001).

Some studies have compared the satellite retrievals with other measurements. Goloub et al. (1999) and Higurashi et al. (2000) have compared AOD and Ångström exponent from satellite retrievals with the global ground-based sun photometer measurements from the Aerosol Robotic Network (AERONET). In Torres et al. (2002) a comparison of AOD from satellite retrieval and from AERONET is performed. Haywood et al. (2001a) compared satellite-retrieved optical depth with optical depth retrieved from aircraft-mounted pyranometers. Further, in Veefkind et al. (1999) satellite retrievals from two different satellite instruments were compared for a smaller region in the Tropical Aerosol Radiative Forcing Observational Experiment (TARFOX) campaign. In general, satellite-retrieved AOD compares well with other observations; however, there are significant uncertainties in the current and past satellite retrievals.

In this study we will compare AOD from four satellite sensors (AVHRR, POLDER, OCTS, and TOMS) for an 8-month period (November 1996 to June 1997). The satellite retrievals of AOD based on the satellite instruments used in this study have been validated previously in separate studies. The ultimate objective of this intercomparison is to explore the satellite aerosol retrievals as a tool to validate global aerosol models. However, an evaluation of the quality of the different retrievals is beyond the scope of this paper. Rather we examine similarities and differences between the five satellite datasets. We also offer a preliminary comparison of each satellite product with ground-based measurements from AERONET sun photometers.

## 2. Satellite retrieval

We have chosen to make a comparison of satellite retrievals in a period from November 1996 to June 1997 during which information is available from several satellite sensors. The data used in our study are documented in the literature. We have based this study on results from four different satellite instruments, namely, AVHRR, POLDER, OCTS, and TOMS, from which global aerosol retrievals over ocean are available. Our analysis covers the 8-month period the OCTS and POLDER instruments onboard the *Advanced Earth Observing Satellite (ADEOS)* were operating. AVHRR data are available from 1981 to the present, and TOMS from 1979 to 1992 and 1996 to the present.

For this study two different retrievals are available for AVHRR (a one-channel retrieval AVHRR-1 and a two-channel retrieval AVHRR-2), and thus we have altogether five retrievals which will be described briefly in the following. For a general outline of remote sensing of aerosols, see King et al. (1999). All five retrievals use lookup tables (LUTs). The way stratospheric aerosols are treated in the retrieval of AOD differs significantly. However, in the period selected here, the stratospheric contribution is minor, as there were no major volcanic eruptions. In this study, we concentrate on comparing AOD only. The Ångström exponent is not available currently in all five products, and it is known to be generally less accurate than AOD. Its accuracy always degrades in inverse proportion to AOD and depends upon two sensor-specific factors: errors in individual channels and spectral separation between the channels (Ignatov et al. 1998; Ignatov 2002; Ignatov and Stowe 2002b).

All five AOD products used in this study are derived from one or two radiometer-specific spectral channels. The AVHRR channels on board National Oceanic and Atmospheric Administration (NOAA) satellites are spectrally very wide, and vary from one NOAA satellite to another. Based on the extensive analyses of the effective wavelengths  $\lambda_{\text{eff}}$  for NOAA-6 through NOAA-16 satellites, Ignatov and Stowe (2002a) proposed that  $\lambda_1 = 630$  nm and  $\lambda_2 = 830$  nm be used to represent a generic AVHRR sensor. POLDER takes measurements at  $\lambda_1 = 670$  nm and  $\lambda_2 = 865$  nm, OCTS at  $\lambda_1 = 667$  nm and  $\lambda_2 = 862$  nm, and TOMS at  $\lambda_1 = 331$  nm and  $\lambda_2 = 360$  nm.

The AOD retrievals are reported at  $\lambda = 500$  nm for OCTS, at  $\lambda = 550$  nm for the AVHRR-2 and TOMS, at  $\lambda = 630$  nm for the AVHRR-1, and at  $\lambda = 865$  nm for POLDER. Ignatov et al. (1995) and Ignatov and Stowe (2002a) argue that the retrievals should be reported as close to the measurement wavelength as practical. If a different reference wavelength is needed, it should be preferably chosen between the measurement wavelengths of  $\lambda_1$  and  $\lambda_2$ , as interpolation is known to be more accurate than extrapolation. Practical considerations suggest, however, that the comparison in our

particular case be done at 550 nm. Therefore, the AVHRR-1, OCTS, and POLDER AODs have been scaled over to 550 nm using the Ångström exponent, derived from AVHRR-2, OCTS, and POLDER, respectively. It should be recognized that in all cases, this is an extrapolation beyond spectral interval of measurements, which may cause additional errors in either product (presumably most important for one-channel retrievals). However, at this time, this source of error is deemed to be relatively small compared to the differences seen between the different products.

The five products are given as monthly averages. All the retrieved AODs are compared on a  $1^\circ \times 1^\circ$  resolution. AVHRR-1 and AVHRR-2, as well as TOMS products, are given in this resolution. POLDER and OCTS products are given on  $0.5^\circ \times 0.5^\circ$  resolution, and we have averaged these onto  $1^\circ \times 1^\circ$ . In the following, a description is given of retrieval procedures for each of the five datasets. Details on how data are mapped from the original retrievals onto the  $1^\circ \times 1^\circ$  or  $0.5^\circ \times 0.5^\circ$  products can be found in this description or in references given there.

#### a. AVHRR-1

In this study we use a subset of *NOAA-14* data from the Pathfinder Atmosphere (PATMOS) AVHRR multi-year (1981–99) multisatellite (*NOAA-7*, *-9*, *-11*, and *-14*) dataset (Stowe et al. 2002; Ignatov and Nalli 2002). Daily PATMOS product includes surface geography, sun-view geometry, and the  $(110 \text{ km})^2$  statistics (mean and standard deviation) of AVHRR radiances, calculated separately for the clear-sky and cloudy fractions of each grid. Cloud screening is done with the Clouds from AVHRR (CLAVR) algorithm, which uses a set of sophisticated tests based upon contrast, and spectral and spatial signatures in the five AVHRR channels (Stowe et al. 1999).

AOD is derived by applying a single channel algorithm to the daily averaged  $(110 \text{ km})^2$  clear-sky reflectance in AVHRR channel 1 (Stowe et al. 1997). A four-dimensional (sun, view, relative azimuth angles, and AOD) lookup table had been precalculated using the Dave radiative transfer model. A nonvariable aerosol model assumes particles to be spherical and nonabsorbing ( $n = 1.40 - 0i$ ), with a monomodal lognormal size distribution (Stowe et al. 1997). A robust single-channel technique is used for PATMOS processing intentionally. The information content of the AVHRR two-channel scheme degrades in inverse proportion to AOD (Ignatov et al. 1998; Ignatov 2002; Ignatov and Stowe 2002b; Ignatov and Nalli 2002). For the  $(110 \text{ km})^2$  PATMOS data, the critical value of AOD at which the advantages of a two-channel scheme over the single-channel one are fully lost, is at  $\tau_0 \sim 0.11$  at  $0.63 \mu\text{m}$  (Ignatov and Nalli 2002), close to typical AOD over oceans.

#### b. AVHRR-2

Mishchenko et al. (1999) and Geogdzhayev et al. (2002) describe a two-channel retrieval from AVHRR. In the most updated version of the retrieval the Ångström exponent is derived in addition to AOD from the retrievals. The two channels used in the algorithm are at 650 and 850 nm. A power-law size distribution is used to describe the size of the aerosols. The aerosols are assumed to absorb solar radiation slightly as a wavelength-independent refractive index of  $1.5 - 0.003i$  is adopted. Further, aerosols are assumed to be spherical. The effective resolution is 30 km based on the International Satellite Cloud Climatology Project (ISCCP) DX dataset (Rossow et al. 1996).

The cloud screening is basically performed with the ISCCP cloud detection scheme (Rossow and Garder 1993). However, the algorithm has been made somewhat more conservative to allow identification of thin cirrus and small cumulus clouds (see Geogdzhayev et al. 2002). In addition, a criterion related to cloud screening is that AOD above 0.6 at higher latitudes than  $50^\circ$  are rejected, and elsewhere a maximum AOD of 1.0 is assumed.

#### c. POLDER

A description of the POLDER aerosol retrieval procedure is given in Goloub et al. (1999) and Deuze et al. (1999, 2000). The algorithm is based on measurements at wavelengths 670 and 865 nm. The optical depth and Ångström exponent are derived and the AOD is given for 865 nm. First the Ångström exponent and subsequently an aerosol model are derived from the spectral and angular dependence of the radiances. Thereafter, the AOD is retrieved. A pixel size of  $6 \text{ km} \times 6 \text{ km}$  is used and  $3 \times 3$  pixels are adopted. The top of the atmosphere reflectances are calculated for a large number of azimuth and zenith angles for different aerosol models and different AOD. Calculations are performed for 12 aerosol models, namely, using four values of the modal radius and three values of the refractive index. A monomodal lognormal size distribution is used. Furthermore, nonabsorbing spherical aerosols are assumed. The algorithm derives only tropospheric aerosols as the retrieval corrects for stratospheric contribution.

In the cloud screening, four criteria are used (Bréon and Colzy 1999). Two use threshold values (including one containing spectral variation) for the 443-nm reflectance, one uses the pressure from two POLDER channels, and finally one uses polarization capabilities.

#### d. OCTS

In Nakajima and Higurashi (1998), Higurashi and Nakajima (1999), and Higurashi et al. (2000), the OCTS aerosol retrieval is described. The resolution of the re-

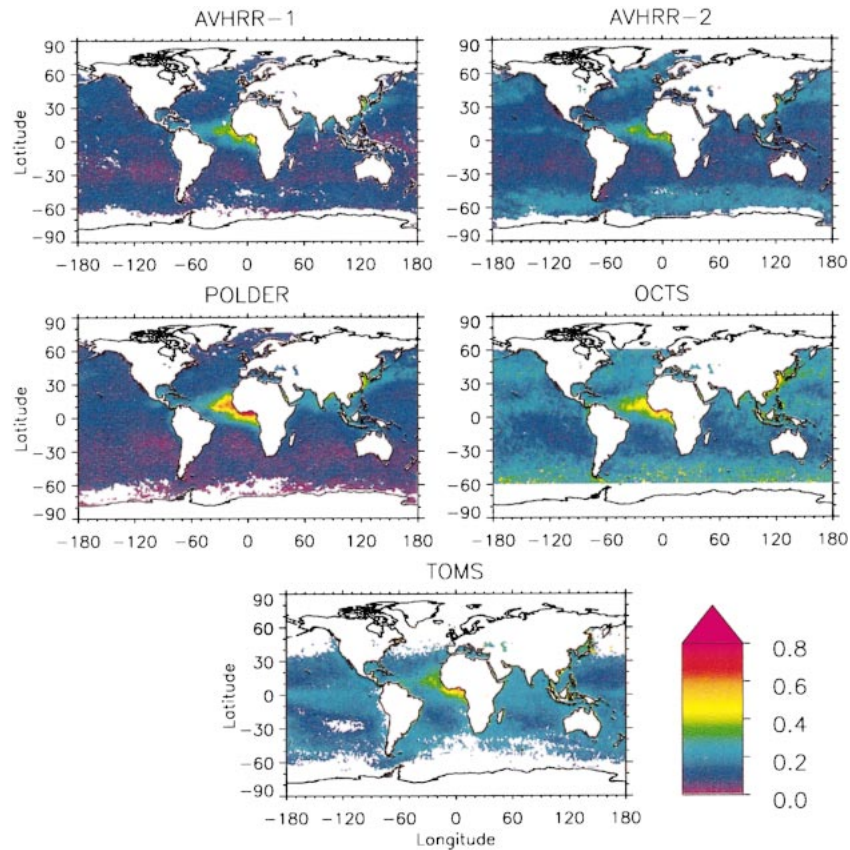


FIG. 1. Averaged AOD (550 nm) over ocean for the period Nov 1996–Jun 1997. Maximum AOD is 0.77, 1.00, 1.21, 1.35, and 1.80, respectively, for AVHRR-1, AVHRR-2, POLDER, OCTS, and TOMS. Values are given with minimum of data for 2 months.

trieved data is  $0.5^\circ \times 0.5^\circ$ , which consists of  $10 \times 10$  pixels. The algorithm uses the two channels at 667 and 862 nm and allows for retrieval of AOD and Ångström exponent. The Ångström exponent is used so that the AOD is converted to 500 nm. A bimodal lognormal size distribution and assumption of spherical particles are used in the algorithm with a complex refractive index of  $1.5 - 0.005i$ , which assumes some absorbing aerosols. The LUT calculations have been performed for many solar and satellite zenith angles, azimuthal angles, and peak ratios in the bimodal size distribution.

The cloud screening is based on threshold values for the reflections in the visible region and the standard deviation in the reflection in the visible region.

#### e. TOMS

The aerosol optical depth retrieval from TOMS is described in Torres et al. (1998, 2002). Measurements from TOMS are based on the near-UV region, and often the aerosol index from TOMS is used (see e.g., Herman et al. 1997; Hsu et al. 1996). The AOD retrieval uses information at two wavelengths in the region 331–360 nm, but they are reported for 380 and 550 nm (converted

as described in Torres et al. 2002). The monthly mean retrieved data are given at  $1^\circ \times 1^\circ$  based on data with rather low resolution ( $40 \text{ km} \times 40 \text{ km}$  in nadir). In addition to retrieval of AOD, one more parameter is retrieved (size or imaginary refractive index) depending on aerosol composition, from which the single scattering albedo is calculated.

The retrieval uses three major aerosol types, and LUT are provided for two datasets (dust–sulfate and sulfate–carbonaceous aerosol models). For the carbonaceous and dust aerosols, three and four aerosols models are used, respectively. All particles are assumed to be spherical.

The cloud screening threshold adopted for reflectivities is 15%. Further, the aerosol index is used in additional cloud screening.

### 3. Global comparison of satellite data

#### a. Global distribution

The global distribution of AOD from the available five datasets is shown for 550 nm as 8-month averages in Fig. 1. Several characteristic features that are also

discussed elsewhere can be seen in the figure (e.g., Husar et al. 1997; Nakajima and Higurashi 1998; Deuze et al. 1999; Tanré et al. 2001). Generally, the AOD is much larger near the continents than over open ocean. The most striking feature is the large AOD west of the mid and northern part of Africa, which is due to wind-blown mineral dust from Sahara and aerosols from biomass burning. The mineral dust influences the radiative balance in this region substantially (Alpert et al. 1998; Haywood et al. 2001b). Along the Asian continent large AOD values are detected by all five retrievals, mainly due to industrial pollution as the Ångström exponent (not shown) is high in this region. Likewise, along the east coast of North America and near the European continent the source of aerosols is mainly from industrial pollution. Biomass burning is the main contributor to the AOD near Central and South America and southern Africa. The most intense biomass burning in the Southern Hemisphere (southern Africa and South America) takes place in August and is not included in the period covered by this analysis. Over large ocean regions away from the coast the AOD is dominated by sea salt aerosols.

The general pattern with higher AOD near the coast is similar in all retrievals. Further, the large maximum due to the mineral dust from Sahara and biomass burning is significant in all five figures. However, the large differences between the retrievals over open ocean are striking. In particular the differences are large at mid-latitudes in the Southern Hemisphere.

Figure 1 suggests that the largest difference between the five retrievals appear to match well with the locations that are known to be generally more cloudy, in particular the high latitudes in both hemispheres, and the intertropical convergence zone. This observation, which seems to be consistent with analyses of cloud effect by Mishchenko et al. (1999) and Ignatov and Nalli (2002), needs further investigation and better understanding. On the one hand, OCTS and TOMS and partly AVHRR-2 may have included some clouds in the aerosol loading, yielding a too-high AOD. On the other hand, AVHRR-1 and POLDER may have interpreted high AOD partly as clouds leading to a too-small AOD. The problem of separating aerosols and clouds is particularly difficult in areas with high thin clouds, as they can have AODs smaller than the cloud detection limits. Further in regions close to clouds and with high winds, the relative humidity can also be very high leading to a large AOD and an inhomogeneous pattern.

Figure 2a shows the average AOD of the five retrievals for the 8-month period yielding much of the same pattern as described above. The standard deviation is shown in Figure 2b, with high values in two major regions, one west of Africa and a second at midlatitudes in the Southern Hemisphere. To determine in which regions the aerosol retrievals are most uncertain, a useful quantity is the ratio of the standard deviation to the mean of the five retrievals. A global distribution of this quan-

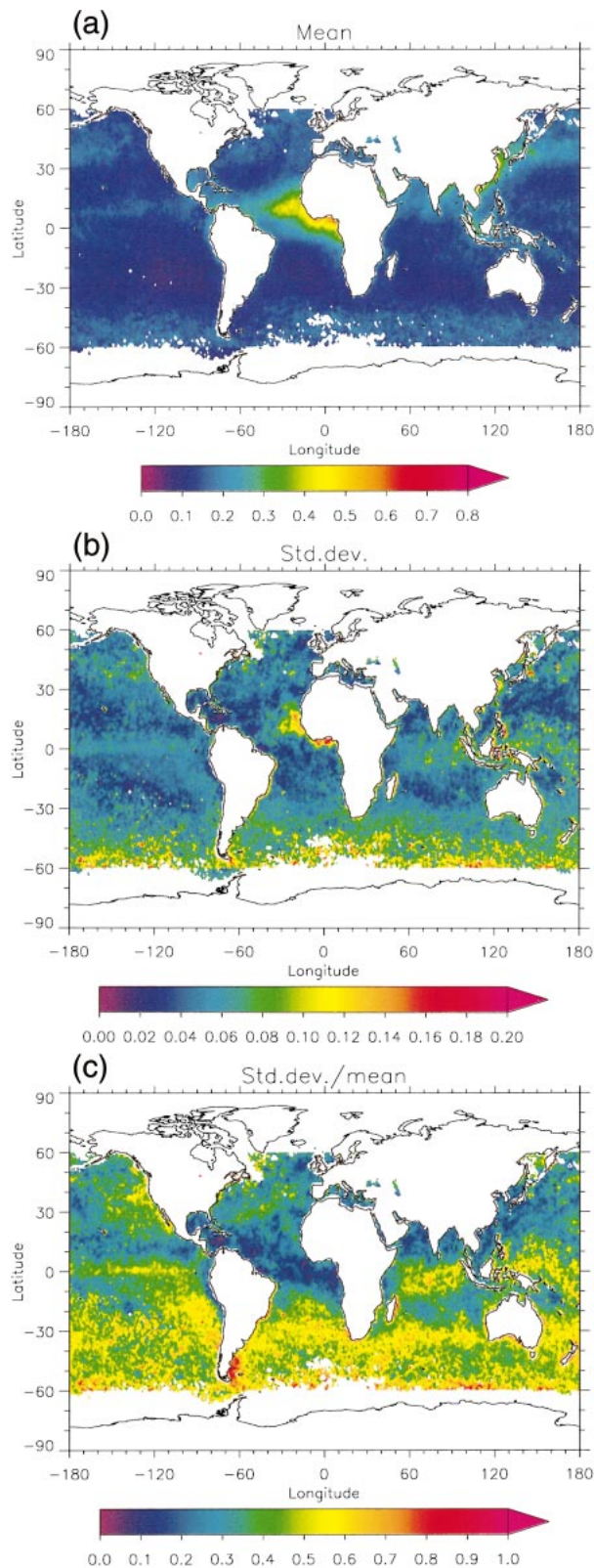


FIG. 2. Averaged statistics for the five aerosol retrievals over the 8-month period: (a) mean (b) standard deviation, and (c) standard deviation divided by the mean. Values are given when at least four retrievals have no missing data.

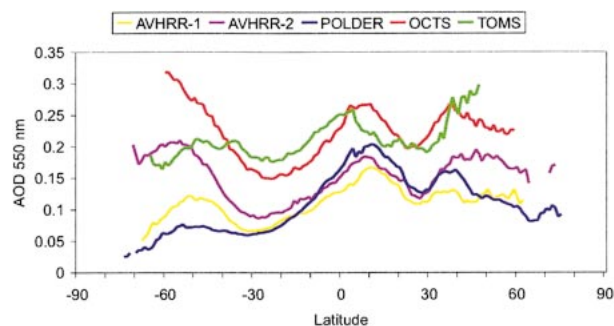


FIG. 3. Zonal mean AOD for the five datasets at 550 nm.

tity is shown in Fig. 2c. Large hemispheric differences are seen. The ratio is particularly large close to 60°S approaching the border beyond which the aerosol retrievals at solar wavelengths cannot be used. In this region few measurements are available and a further complicating factor is the high amount of clouds in this region. Around 30°S, high values can also be seen in the figure, in a region with generally very low AOD. West of Africa the standard deviation was high as well as the mean AOD. However, the ratio of these two is low in this region, indicating that the relative uncertainties in the aerosol retrievals is not particularly large here.

The zonal mean of the AOD is shown in Fig. 3. The range in the AOD is substantial, with AVHRR-1 and POLDER generally having the lowest values, and OCTS and TOMS the highest AOD. However, it is clear that none of the retrievals have AOD consistently higher or lower than the others. As in Fig. 2, we see the largest uncertainties at high latitudes in the Southern Hemisphere also in Fig. 3. Despite the large range in the results, the zonal pattern is much more similar.

#### b. Regional comparison

Figure 4 shows the global, Southern Hemisphere, and Northern Hemisphere mean AOD over ocean over the period from November 1996 to June 1997, represented by monthly means.

Except for the first 3 months, the Northern Hemisphere AOD is significantly higher than the one in the Southern Hemisphere. Generally, on one side TOMS and OCTS and on the other side AVHRR-1 and POLDER have rather similar AOD for global, Northern Hemisphere, and Southern Hemisphere mean. Mostly, AVHRR-2 has AODs between the two groups. The AOD from TOMS and OCTS is up to a factor of 2 higher than the AOD from AVHRR-1 and POLDER. The smallest difference is in the latter few months in the Northern Hemisphere. The monthly variation is remarkably small compared to the differences between the retrievals.

In Fig. 5 the AOD over ocean is split into five large oceanic regions. Similar to what is shown in Fig. 2, the

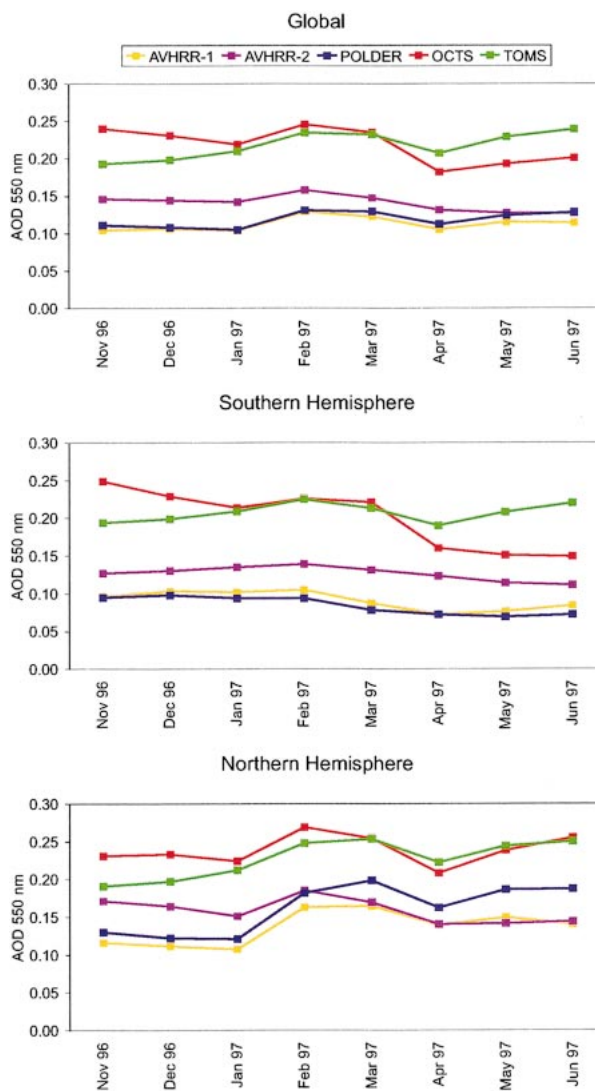


FIG. 4. (top) Global, (middle) Southern Hemisphere, and (bottom) Northern Hemisphere mean AOD (550 nm) over ocean (monthly averages).

OCTS and TOMS have much higher AODs than AVHRR-1 and POLDER in all the regions. In the Antarctic ocean region, AVHRR-2 values are closer to OCTS and TOMS, whereas for the four other oceanic regions they are closer to AVHRR-1 and POLDER. The spread in the AOD values is particularly large in the Antarctic ocean region and smallest in the North Atlantic Ocean.

Table 1 shows the 8-month mean for the five aerosol retrievals for global, Southern Hemisphere, and Northern Hemisphere mean, as well as for the five oceanic regions. The table illustrates that there is at least a factor of 2 difference in the AOD between the retrievals, even at a global scale, and a factor of 3 difference in the Antarctic ocean region.

Figure 6 shows a comparison of the five satellite re-

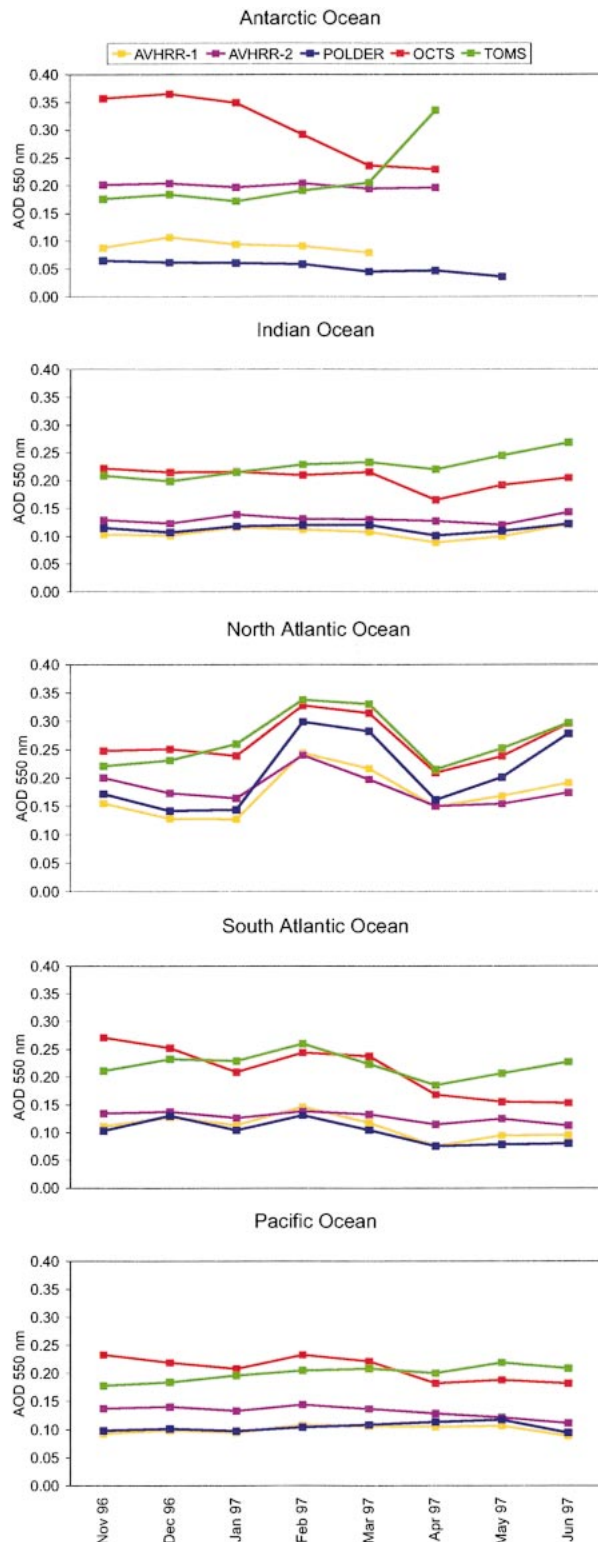


FIG. 5. As Fig. 4, but for five ocean regions.

trievals over 11 smaller oceanic regions close to continents. This figure shows a more complex pattern of the five sets with AODs than what is apparent in Figs. 4 and 5. Overall, there is a better agreement between the aerosol retrievals in the regions close to the continents compared to the larger regions. At the Cape Verde plateau and in certain months at the Arabian Sea, the Bay of Bengal, the Red Sea, the East China Sea, and the Sea of Japan, the POLDER AODs are highest; in the other regions TOMS or OCTS have the highest values. There is mainly a factor of 2 difference between the highest and the lowest AOD. The seasonal variations are very similar for the five retrievals. The January 1997 TOMS data for the eastern coast of United States, Black Sea, and Caspian Sea are based on very poor statistics and therefore excluded in the figure. At this time of year at mid- and high latitudes, snow/ice and cloud contamination is very severe in the TOMS data.

To summarize the comparison of the five datasets, we show scatterplots of AOD over ocean for various combinations of the retrievals. The results are shown in Fig. 7 for 10 combinations of the datasets. The scatterplot where the majority of the points follow the 1-to-1 line closest is for AVHRR-1 versus POLDER. For OCTS versus TOMS, AVHRR-2 versus TOMS, and AVHRR-2 versus OCTS, the scatter is substantial, especially for high AODs.

In several of the scatterplots, a bimodal distribution is evident (POLDER versus OCTS, AVHRR-1 versus OCTS, POLDER versus TOMS, and partly AVHRR-1 versus AVHRR-2, AVHRR-1 versus TOMS, and AVHRR-2 versus POLDER). The mode with much larger values for TOMS, OCTS, and partly AVHRR-2 than AVHRR-1 and POLDER is mainly owing to differences south of 25°S, as can also be seen in Fig. 1. Another feature that can be seen in Fig. 7 is that OCTS and TOMS (and partly AVHRR-2) have few retrievals of AOD below 0.05.

#### 4. Comparison between satellite and AERONET data

The AERONET is a ground-based worldwide station network that consists of a large number of sun photometers (Holben et al. 1998). The AERONET dataset is independent of satellite retrievals, but it is used as ground validation of some satellite data. The AOD from the satellite retrievals are here compared to AOD from the AERONET for some selected islands and coastal stations. The AERONET stations used for this comparison are shown in Table 2.

A comparison of satellite-retrieved AOD at 550 nm and AERONET AOD mean of 440 nm (some few at 500 nm) and 670 nm are shown in Fig. 8 for AERONET stations with more than 1 month of observations. Monthly mean data for AERONET is generated as average of the daily mean of the available days with measurements. In general the agreement between the sat-

TABLE 1. Eight-month average AOD for the five aerosol retrievals.

	AVHRR-1	AVHRR-2	POLDER	OCTS	TOMS
Global	0.112	0.140	0.119	0.218	0.218
Southern Hemisphere	0.091	0.126	0.084	0.200	0.207
Northern Hemisphere	0.136	0.158	0.161	0.239	0.227
Antarctic Ocean	0.092	0.199	0.054	0.305	0.211
Indian Ocean	0.106	0.130	0.114	0.205	0.227
North Atlantic Ocean	0.172	0.182	0.210	0.265	0.268
South Atlantic Ocean	0.110	0.127	0.101	0.211	0.222
Pacific Ocean	0.099	0.131	0.104	0.208	0.200

ellite retrievals and AERONET is good, even for stations with seasonal variations. At Barbados and Cape Verde the AOD from the sun photometers is within the range of the AOD from the satellite retrievals and none

of the satellite retrievals differ substantially from the ground-based measurements. At Crete and Lanai there are indications that the satellite retrievals underestimate and overestimate the AOD compared to sun photome-

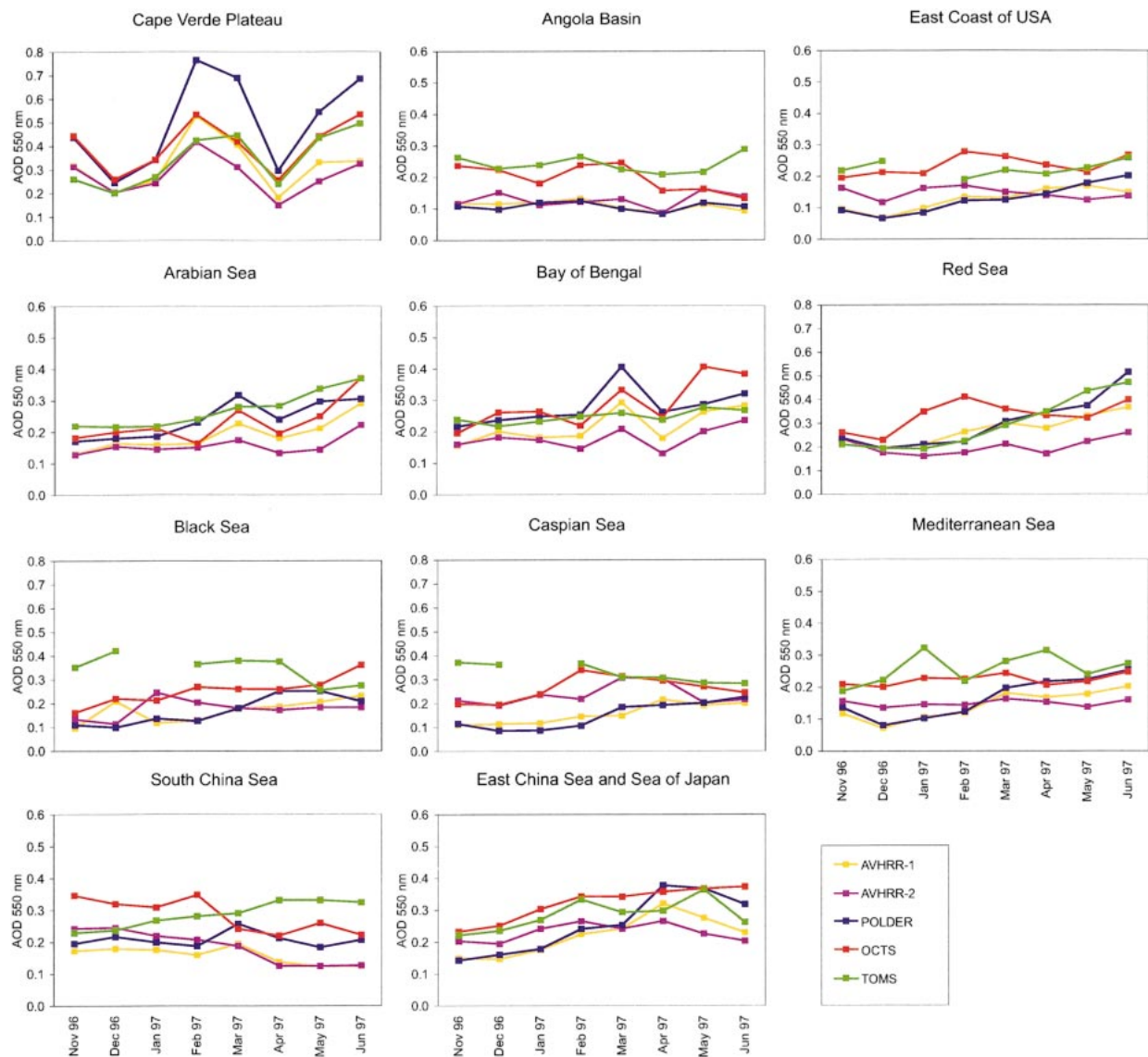


FIG. 6. As Fig. 4, but for 11 near-coastal oceanic regions. Note the different y axis for the Cape Verde plateau, the Red Sea, the Black Sea, and the Caspian Sea.

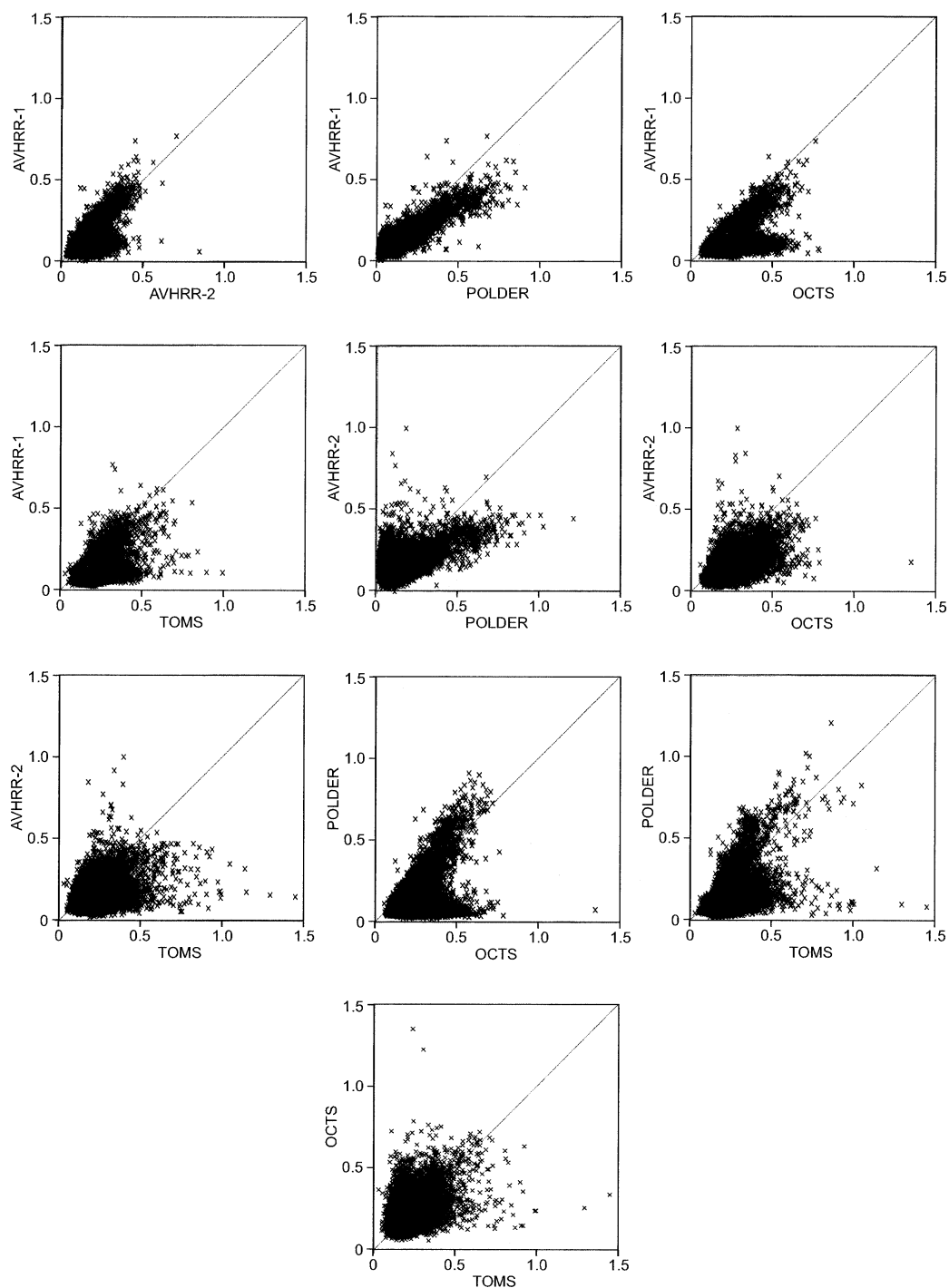


FIG. 7. Scatterplots of pairs of AOD data, mean values for the 8-month period Nov 1996 to Jun 1997, from the five satellite instruments. All data (globally) are included in the analysis.

ters, respectively. For the rest of the stations there are only small periods with large deviations.

A comparison of monthly mean AOD from satellites and ground-based measurements must be interpreted with caution as the number of measurements

can be low and the measurements are not necessarily made at the same time nor even at the same days (Ichoku et al. 2002). In the AERONET data, the frequency of measurements is particularly low at Male in November 1996 with only 1 day with observations.

TABLE 2. AERONET stations used in the analyses in this work.

Station name	Latitude	Longitude	Altitude (m)
Ascension Island	07°58'S	14°24'W	30
Barbados	13°10'N	59°30'W	0
Bermuda	32°22'N	64°41'W	10
Capo Verde	16°43'N	22°56'W	60
Cheritan	37°16'N	75°25'W	0
Crete	35°20'N	25°40'E	140
Dakar	14°23'N	16°57'W	0
Dry Tortugas	24°36'N	82°47'W	0
Lanai	20°49'N	156°59'W	80
Male	04°11'N	73°31'E	2
Rame Head	50°21'N	04°08'W	0
Tenerife	28°01'N	16°37'W	10
Zenith	37°21'N	70°00'W	0

For the rest of the stations, the number of days with observations within a month are mostly above 15. The wavelength dependence of the AOD in the AERONET data is generally small, except at Rame Head and Crete with more influence by industrial pollution and smaller particles.

Figure 9 shows a scatterplot of monthly mean AOD for AERONET and each of the satellite retrievals. Data for all the stations listed in Table 2 are used in the analysis. There is a tendency for the aerosol satellite retrievals to have higher AODs than the AOD from the sun photometers for low AOD and vice versa for high AODs. The highest AOD is often from Cape Verde and Dakar. The high regression intercept results from non-aerosol effects (Ignatov et al. 1995). First, the coastal

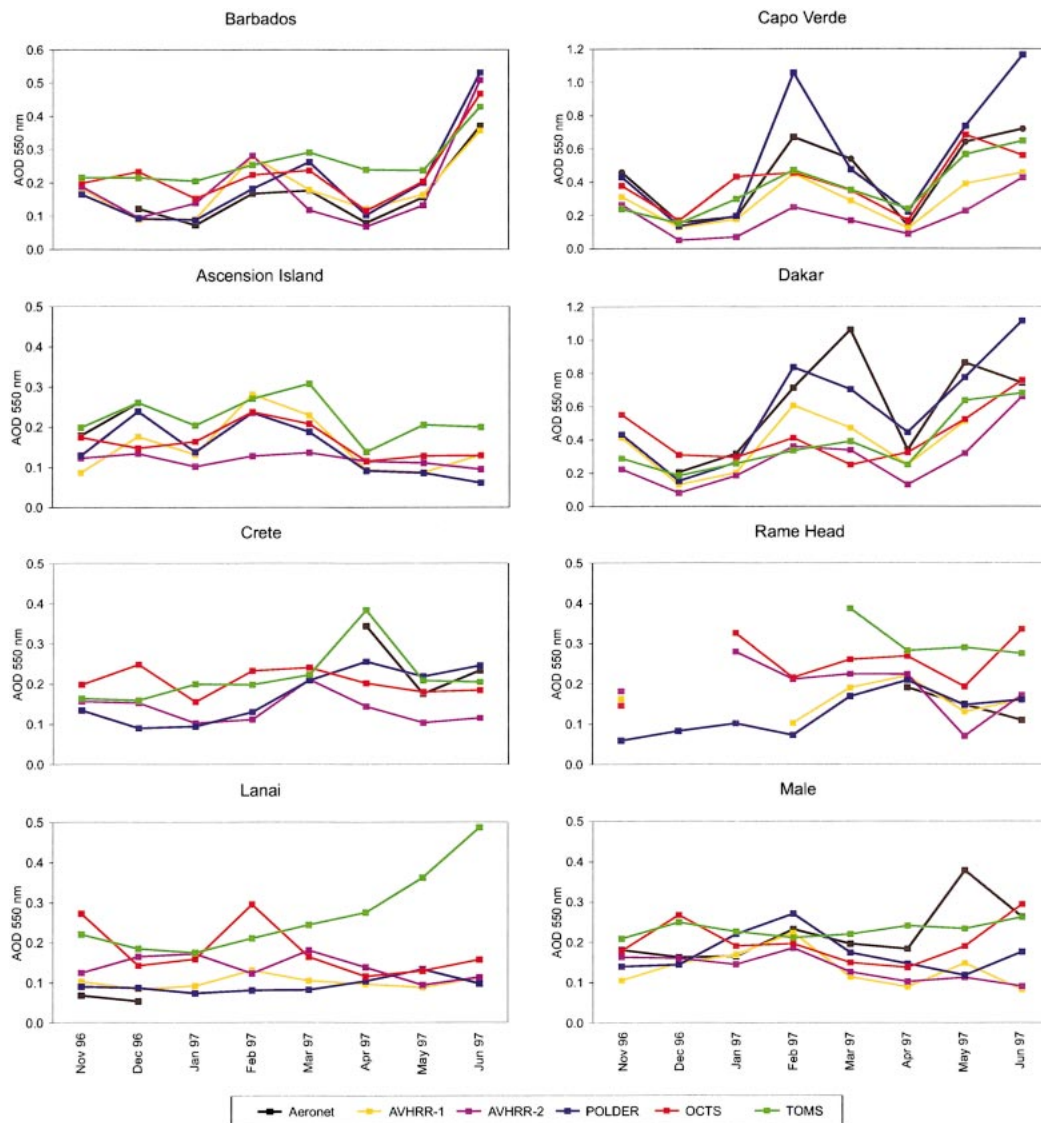


FIG. 8. AOD from AERONET, as well as the five satellite retrievals. Data represent monthly mean values. The satellite data are for 550 nm, while the AERONET data are mean values of AOD at 440 and 670 nm (500 and 670 nm at Ascension Island, Male, and Lanai). Note the different AOD scales for the various stations.

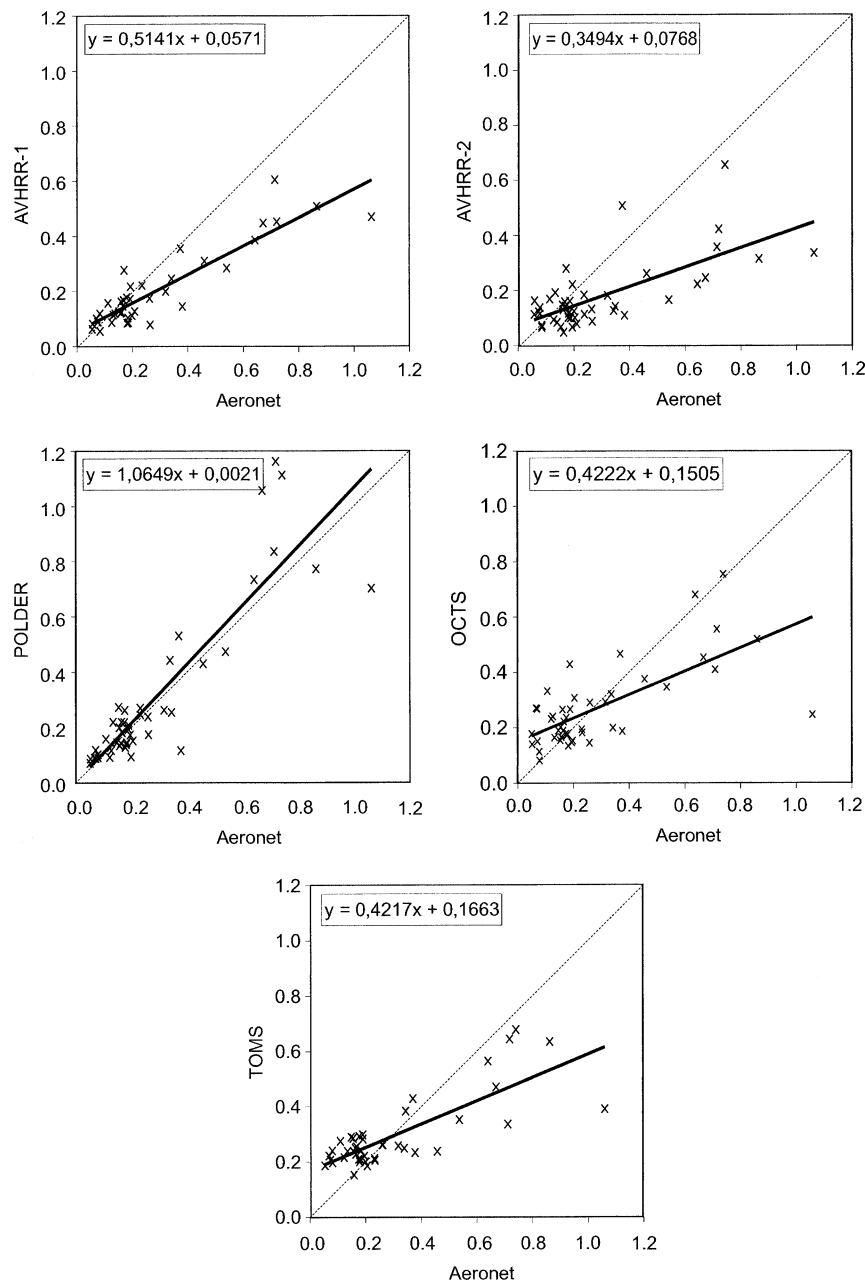


FIG. 9. Scatterplot of monthly mean AOD, the AERONET data vs each of the five satellite retrievals. Satellite data at 550 nm, AERONET data mean of 440 (500) and 670 nm.

waters tend to be more turbid and bright than the open ocean. A globally tuned algorithm interprets the larger satellite signal here as an elevated AOD. Second, residual (partial) cloud may still persist in the “cloud-free” satellite radiances used for aerosol retrievals. The relative proportion of these two factors is different in the different AOD products, depending upon their respective cloud screening, spatial resolution, and allowed proximity of the retrievals to the coastal line. For the five products used here, the regression intercept ranges

from +0.002 (POLDER) to 0.17 (TOMS). At high AOD, the accuracy of the retrievals chiefly depends on the aerosol model used (Ignatov et al. 1995). It is this AOD domain where the advantage of a two-channel retrieval, in which the aerosol model is estimated in situ, is expected to be most significant and clearly seen compared to a single-channel scheme with a prescribed aerosol model, such as used in AVHRR-1. However, high AOD values are often due to dust, which introduces problems related to nonsphericity (see section 5). The

POLDER data are in general in better agreement with the AERONET data than the other; however, for large AOD there is substantial scatter between AERONET and POLDER data.

## 5. Discussion and summary

In current satellite retrievals of aerosols, which normally assume spherical particles, there are at least five unknown quantities. The five quantities are the AOD, two parameters describing the size distribution, for example, geometric mean radius and geometric standard deviation for a lognormal size distribution, and finally the real and imaginary refractive index. In a two-channel (one channel) retrieval two (one) of these quantities can be determined, whereas for the other quantities, assumptions must be made. Some of the channels used in the retrievals are in spectral regions with gas absorption, which for some gases varies spatially and temporally. The ocean surface reflectance is another source of uncertainty in remote sensing of aerosols. A further uncertainty is the altitude of the aerosol layer, in particular for absorbing aerosols in the TOMS retrieval. In addition to these uncertainties, the quality of satellite data used for aerosol retrievals may play a significant role. Radiometric errors (calibration, noise, digitization) are important when working with small signals used in aerosol remote sensing. The largest source of uncertainty in the aerosol retrieval is most likely the cloud screening.

In this study we have compared five different aerosol retrievals (including both one-channel and two-channel algorithms) over global ocean from four different satellite instruments for monthly mean AOD for an 8-month period. From what is described in the previous paragraph, it is clearly a difficult task to retrieve AOD from satellites. It is therefore reasonable to find large differences in AOD from the different algorithms. The difference in the AOD in the five retrievals is at least a factor of 2 between the one giving the lowest to the one giving the highest value. Overall, the algorithms produce similar results close to continents where the AOD often is relatively high. The largest uncertainties in the results are in the Southern Hemisphere, and in particular in the Pacific Ocean and Antarctic Ocean region far from continents. In general, the OCTS and TOMS have the highest AOD, and POLDER and AVHRR-1 the lowest AOD, with AVHRR-2 often in between the two groups, but closer to the lowest ones. Closer to continents this ranking differs somewhat and, for example, in the Cape Verde plateau POLDER has the highest AODs.

The two-channel algorithms OCTS, POLDER, and AVHRR-2 have many similarities. The OCTS and POLDER instruments were on the same satellite. The retrieval adopting the information from TOMS also uses two channels, but at shorter wavelengths (in the UV region). AVHRR-2 and AVHRR-1 use data from the same instrument but differ in their calibration and cloud

screening, number of channels, and retrieval algorithm assumptions (aerosol model, surface reflectance, and gaseous absorption). As expected there are many similarities between the various datasets. More surprisingly, we have identified also major differences between the results of the five different aerosol retrievals. We have not attempted to judge the quality of the various datasets. In fact what our study shows is that there is in general no obvious difference in their quality. There is no single dataset that stands out as very different from the others. We suspect that much of the differences can be attributed to the complexity of cloud screening as most of the largest relative differences are found in regions with large cloud cover, this is particularly a problem at high latitudes in the Southern Hemisphere. Some of the retrievals may identify large AOD as clouds such as POLDER and AVHRR-1, whereas TOMS and OCTS may have less restrictive screening criteria. Haywood et al. (1997) and Myhre et al. (2002) show that small-scale variation in relative humidity can influence the radiative effects of hygroscopic aerosols substantially. High relative humidity may therefore increase the AOD of sea salt aerosol substantially. It therefore has the potential to be confused with optically thin clouds and fog at low levels. In other regions, as west of Sahara, where AOD values are generally high in all datasets, other issues in the aerosol retrievals (including cloud screening) would influence the differences in the results.

The aerosol retrievals are based on instruments on three satellites, which are nonsynchronous in time. Kaufman et al. (2000) show that the diurnal variation in the AOD is small, and that data acquisition during the day is therefore rather insignificant by using a large number of AERONET measurements. However, it cannot be ruled out that this problem could, to a limited extent, contribute to the differences between the datasets.

The PATMOS AOD is known to have deficiencies (Ignatov and Stowe 2002b; Ignatov and Nalli 2002). In particular, using a more accurate and up-to-date 6S radiative transfer model (Vermote et al. 1997) in place of Dave (Ignatov and Stowe 2002a) suggests that the current Dave-based PATMOS AOD is biased low. The adjustment is a complicated function of AOD itself (Ignatov and Nalli 2002), but on average it is  $+3.5 \times 10^{-2}$  for the NOAA-14 period. Also, the calibration by Rao and Chen (1999) used in PATMOS, may be biased low by 4.5%–8.5% (Tahnk and Coakley 2001; Nguyen et al. 2002, manuscript submitted to *J. Atmos. Oceanic Technol.*), which would further raise AVHRR-1 AOD by approximately  $2.4 \times 10^{-2}$  (Ignatov 2002).

All the aerosol retrievals assume spherical particles, but several studies have shown that nonsphericity may have a substantial impact (Mishchenko et al. 1995, 1997; Dubovik et al. 2002; Mishchenko et al. 2003, hereafter MIS). Dubovik et al. (2002) found that using nonspherical particles significantly improved the retrieval from AERONET measurements. Further, MIS

used laboratory measurements of the phase function for natural mineral aerosols to show that the AVHRR retrieval strongly underestimated the AOD of dustlike particles.

We have further compared the AOD from the five satellite retrievals with AERONET data. The AERONET stations are in regions where the agreement between the retrievals is generally good, and the satellite data are also mostly in reasonable agreement with the AERONET data. The seasonal variation is also well reproduced. The results of MIS show that for dustlike particles, the assumption of spherical particles may explain a general underestimation of AOD from satellite retrievals compared to the AERONET observations for high AODs. Furthermore, comparison of monthly mean satellite and AERONET retrievals of AOD must be interpreted with caution as time and number of available retrievals can be different.

In global aerosol modeling there is clearly a need to use satellite data in the validation. In such validation monthly mean data are often preferred since there is a limited spatial coverage of the satellite data for single days and since many global models do not use realistic meteorological data, which is necessary for a useful comparison on a daily basis. However, in follow-up studies, single-day data for selected periods should be used. This is needed in order to understand and explain the differences between the results from the various algorithms in detail. It will also allow comparison with models using realistic meteorological data. Finally, it would allow a better and more realistic comparison with the AERONET data. In such comparisons, the wavelength dependence of the AOD could be investigated more closely. This has the potential to give useful information about the size distributions.

To better understand the differences between the retrievals, further comparison with ground-based or aircraft measurements should be performed. In particular there should be increased effort in the validation in regions with largest uncertainties, such as in the Southern Hemisphere in the Pacific Ocean and the Antarctic, based on aerosol campaigns or permanent sun photometers on islands in this region. New satellite instruments designed for aerosol retrieval, such as the Moderate-Resolution Imaging Spectroradiometer (MODIS) and the Multiangle Imaging Spectroradiometer (MISR), will probably also improve the remote sensing of aerosols over ocean substantially in addition to providing much information over land.

**Acknowledgments.** We acknowledge the principle investigators Chuck McClain, Ken Voss, and Samantha Lavender for use of data from their AERONET sites. POLDER is a joint CNES/NASDA effort. Information on POLDER can be found online at <http://earth-sciences.cnes.fr/POLDER/>

## REFERENCES

- Alpert, P., Y. J. Kaufman, Y. Shay-El, D. Tanre, A. da Silva, S. Schubert, and J. H. Joseph, 1998: Quantification of dust-forced heating of the lower troposphere. *Nature*, **395**, 367–370.
- Boucher, O., and D. Tanre, 2000: Estimation of the aerosol perturbation to the earth's radiative budget over oceans using POLDER satellite aerosol retrievals. *Geophys. Res. Lett.*, **27**, 1103–1106.
- Bréon, F.-M., and S. Colzy, 1999: Cloud detection from the spaceborne POLDER instrument and validation against surface synoptic observations. *J. Appl. Meteor.*, **38**, 777–785.
- Chin, M., and Coauthors, 2002: Tropospheric aerosol optical thickness from the GOCART model and comparisons with satellite and sun photometer measurements. *J. Atmos. Sci.*, **59**, 461–483.
- Chu, D. A., Y. J. Kaufman, C. Ichoku, L. A. Remer, D. Tanré, and B. N. Holben, 2002: Validation of MODIS aerosol optical depth over land. *Geophys. Res. Lett.*, **29**, 1–4.
- Deuzé, J. L., M. Herman, P. Goloub, D. Tanré, and A. Marchand, 1999: Characterization of aerosols over ocean from POLDER/ADEOS-1. *Geophys. Res. Lett.*, **26**, 1421–1424.
- , P. Goloub, M. Herman, A. Marchand, G. Perry, S. Susana, and D. Tanré, 2000: Estimate of the aerosol properties over the ocean with POLDER. *J. Geophys. Res.*, **105**, 15 329–15 346.
- , and Coauthors, 2001: Remote sensing of aerosols over land surfaces from POLDER-ADEOS-1 polarized measurements. *J. Geophys. Res.*, **106**, 4913–4926.
- Dubovik, O., B. Holben, T. F. Eck, A. Smirnov, Y. J. Kaufman, M. D. King, D. Tanré, and I. Slutsker, 2002: Variability of absorption and optical properties of key aerosol types observed in worldwide locations. *J. Atmos. Sci.*, **59**, 590–608.
- Geogdzhayev, I. V., M. I. Mishchenko, W. B. Rossow, B. Cairns, and A. A. Lacis, 2002: Global two-channel AVHRR retrievals of aerosol properties of the ocean for the period of NOAA-9 observations and preliminary retrievals using NOAA-7 and NOAA-11 data. *J. Atmos. Sci.*, **59**, 262–278.
- Goloub, P., D. Tanré, J. L. Deuzé, M. Herman, A. Marchand, and F. M. Breon, 1999: Validation of the first algorithm applied for deriving the aerosol properties over the ocean using the POLDER ADEOS measurements. *IEEE Trans. Geosci. Remote Sens.*, **37**, 1586–1596.
- Gonzalez, C. R., J. P. Veefkind, and G. de Leeuw, 2000: Aerosol optical depth over Europe in August 1997 derived from ATSR-2 data. *Geophys. Res. Lett.*, **27**, 955–958.
- Haywood, J. M., V. Ramaswamy, and L. J. Donner, 1997: A limited-area-model case study of the effects of sub-grid scale variations in relative humidity and cloud upon the direct radiative forcing of sulfate aerosol. *Geophys. Res. Lett.*, **24**, 143–146.
- , —, and B. J. Soden, 1999: Tropospheric aerosol climate forcing in clear-sky satellite observations over the oceans. *Science*, **283**, 1299–1303.
- , P. N. Francis, I. Geogdzhayev, M. Mishchenko, and R. Frey, 2001a: Comparison of Saharan dust aerosol optical depths retrieved using aircraft mounted pyranometers and 2-channel AVHRR algorithms. *Geophys. Res. Lett.*, **28**, 2393–2396.
- , —, M. D. Glew, and J. P. Taylor, 2001b: Optical properties and direct radiative effect of Saharan dust: A case study of two Saharan dust outbreaks using aircraft data. *J. Geophys. Res.*, **106**, 18 417–18 430.
- Herman, J. R., P. K. Bhartia, O. Torres, C. Hsu, C. Seftor, and E. Celarier, 1997: Global distributions of UV-absorbing aerosols from Nimbus 7/TOMS data. *J. Geophys. Res.*, **102**, 16 911–16 922.
- Higurashi, A., and T. Nakajima, 1999: Development of a two-channel aerosol retrieval algorithm on a global scale using NOAA AVHRR. *J. Atmos. Sci.*, **56**, 924–941.
- , —, B. N. Holben, A. Smirnov, R. Frouin, and B. Chatenet, 2000: A study of global aerosol optical climatology with two-channel AVHRR remote sensing. *J. Climate*, **13**, 2011–2027.

- Holben, B. N., and Coauthors, 1998: AERONET: A federated instrument network and data archive for aerosol characterization. *Remote Sens. Environ.*, **66**, 1–16.
- Houghton, J. T., Y. Ding, D. J. Griggs, M. Noguer, P. J. van der Linden, X. Dai, K. Maskell, and C. A. Johnson, Eds., 2001: *Climate Change 2001: The Scientific Basis*. Cambridge University Press, 98 pp.
- Hsu, N. C., and Coauthors, 1996: Detection of biomass burning smoke from TOMS measurements. *Geophys. Res. Lett.*, **23**, 745–748.
- Husar, R. B., J. M. Prospero, and L. L. Stowe, 1997: Characterization of tropospheric aerosols over the oceans with the NOAA advanced very high resolution radiometer optical thickness operational product. *J. Geophys. Res.*, **102**, 16 889–16 909.
- Ichoku, C., A. Chu, S. Mattoo, Y. Kaufman, L. Remer, D. Tanré, I. Slutsker, and B. Holben, 2002: A spatio-temporal approach for global validation and analysis of MODIS aerosol products. *Geophys. Res. Lett.*, **29**, 8006, doi:10.1029/2001GL013206.
- Ignatov, A., 2002: Sensitivity and information content of aerosol retrievals from AVHRR: Radiometric factors. *Appl. Opt.*, **46**, 991–1011.
- , and N. Nalli, 2002: Aerosol retrievals from multiyear multisatellite AVHRR Pathfinder atmosphere (PATMOS) dataset for correcting remotely sensed sea surface temperatures. *J. Atmos. Oceanic Technol.*, **12**, 1986–2008.
- , and L. Stowe, 2002a: Aerosol retrievals from individual AVHRR channels. Part I: Retrieval algorithm and transition from Dave to 6S radiative transfer model. *J. Atmos. Sci.*, **59**, 313–334.
- , and —, 2002b: Aerosol retrievals from individual AVHRR channels. Part II: Quality control, probability distribution functions, information content, and consistency checks of retrievals. *J. Atmos. Sci.*, **59**, 335–362.
- , —, S. Sakerin, and G. Korotaev, 1995: Validation of the NOAA/NESDIS satellite aerosol product over the North Atlantic in 1989. *J. Geophys. Res.*, **100**, 5123–5132.
- , —, and R. Singh, 1998: Sensitivity study of the Angstrom exponent derived from AVHRR over oceans. *Adv. Space Res.*, **21**, 439–442.
- Kahn, R., P. Banerjee, D. McDonald, and D. Diner, 1998: Sensitivity of multiangle imaging to aerosol optical depth and to pure-particle size distribution and composition over oceans. *J. Geophys. Res.*, **103**, 32 195–32 213.
- Kaufman, Y., R. Fraser, and R. Ferrare, 1990: Satellite measurements of large-scale air pollution: Methods. *J. Geophys. Res.*, **95**, 9895–9909.
- , and Coauthors, 1997: Passive remote sensing of tropospheric aerosol and atmospheric correction for the aerosol effect. *J. Geophys. Res.*, **102**, 16 815–16 830.
- , B. N. Holben, D. Tanré, I. Slutsker, A. Smirnov, and T. F. Eck, 2000: Will aerosol measurements from Terra and Aqua polar orbiting satellites represent the daily aerosol abundance and properties? *Geophys. Res. Lett.*, **27**, 3861–3864.
- King, M. D., Y. J. Kaufman, D. Tanré, and T. Nakajima, 1999: Remote sensing of tropospheric aerosols from space: Past, present, and future. *Bull. Amer. Meteor. Soc.*, **80**, 2229–2259.
- Kuang, Z., and Y. L. Yung, 2000: Reflectivity variations off the Peru Coast: Evidence for indirect effect of anthropogenic sulfate aerosols on clouds. *Geophys. Res. Lett.*, **27**, 2501–2504.
- Mishchenko, M. I., A. A. Lacis, B. E. Carlson, and L. D. Travis, 1995: Nonsphericity of dust-like tropospheric aerosols: Implications for aerosol remote sensing and climate modeling. *Geophys. Res. Lett.*, **22**, 1077–1080.
- , L. D. Travis, R. A. Kahn, and R. A. West, 1997: Modeling phase functions for dustlike tropospheric aerosols using a shape mixture of randomly oriented polydisperse spheroids. *J. Geophys. Res.*, **102**, 16 831–16 847.
- , I. V. Geogdzhayev, B. Cairns, W. B. Rossow, and A. A. Lacis, 1999: Aerosol retrievals over the ocean by use of channels 1 and 2 AVHRR data: Sensitivity analysis and preliminary results. *Appl. Opt.*, **38**, 7325–7341.
- , J. Penner, and D. Anderson, 2002: Global aerosol climatology project. *J. Atmos. Sci.*, **59**, 249.
- , and Coauthors, 2003: Aerosol retrievals from AVHRR radiances: Effects of particle nonsphericity and absorption and an updated long-term global climatology of aerosol properties. *J. Quant. Spectrosc. Radiat. Transfer*, **79–80**, 953–972.
- Myhre, G., J. E. Jonson, J. Bartnicki, F. Stordal, and K. P. Shine, 2002: Role of spatial and temporal variations in the computation of radiative forcing due to sulphate aerosols: A regional study. *Quart. J. Roy. Meteor. Soc.*, **128**, 973–989.
- Nakajima, T., and A. Higurashi, 1998: A use of two-channel radiances for an aerosol characterization from space. *Geophys. Res. Lett.*, **25**, 3815–3818.
- , —, K. Kawamoto, and J. E. Penner, 2001: A possible correlation between satellite-derived cloud and aerosol microphysical parameters. *Geophys. Res. Lett.*, **28**, 1171–1174.
- Penner, J. E., and Coauthors, 2002: A comparison of model- and satellite-derived aerosol optical depth and reflectivity. *J. Atmos. Sci.*, **59**, 441–460.
- Rao, N., and J. Chen, 1999: Revised post-launch calibration of the visible and near-IR channels of AVHRR onboard the NOAA-14 spacecraft. *Int. J. Remote Sens.*, **20**, 3485–3491.
- Rosenfeld, D., 2000: Suppression of rain and snow by urban and industrial air pollution. *Science*, **287**, 1793–1796.
- Rossow, W. B., and L. C. Garder, 1993: Cloud detection using satellite measurements of infrared and visible radiances for ISCCP. *J. Climate*, **6**, 2341–2369.
- , A. Walker, and M. Roiter, 1996: International Satellite Cloud Climatology Project (ISCCP) description of reduced resolution radiance data. WMO/TD-No. 58, World Meteorological Organization, 163 pp.
- Stowe, L. L., A. M. Ignatov, and R. R. Singh, 1997: Development, validation, and potential enhancements to the second generation operational aerosol product at the National Environmental Satellite, Data, and Information Service of the National Oceanic and Atmospheric Administration. *J. Geophys. Res.*, **102**, 16 923–16 934.
- , P. Davis, and P. McClain, 1999: Scientific basis and initial evaluation of the CLAVR-1 global clear/cloud classification algorithm for AVHRR. *J. Atmos. Oceanic Technol.*, **16**, 656–681.
- , H. Jacobowitz, G. Ohring, K. Knapp, and N. Nalli, 2002: The AVHRR Pathfinder Atmosphere (PATMOS) climate dataset: Initial analyses and evaluation. *J. Climate*, **15**, 1243–1260.
- Tahnk, W., and J. Coakley, 2001: Updated calibration coefficients for NOAA-14 AVHRR channels 1 and 2. *Int. J. Remote Sens.*, **22**, 3053–3057.
- Takemura, T., H. Okamoto, Y. Maruyama, A. Numaguti, A. Higurashi, and T. Nakajima, 2000: Global three-dimensional simulation of aerosol optical thickness distribution of various origins. *J. Geophys. Res.*, **105**, 17 853–17 873.
- Tanré, D., F. M. Bréon, J. L. Deuzé, M. Herman, P. Goloub, F. Nadal, and A. Marchand, 2001: Global observation of anthropogenic aerosols from satellite. *Geophys. Res. Lett.*, **28**, 4555–4558.
- Torres, O., P. K. Bhartia, J. R. Herman, Z. Ahmad, and J. Gleason, 1998: Derivation of aerosol properties from satellite measurements of backscattered ultraviolet radiation: Theoretical basis. *J. Geophys. Res.*, **103**, 17 099–17 110.
- , —, —, A. Sinyuk, P. Ginoux, and B. Holben, 2002: A long-term record of aerosol optical depth from TOMS observations and comparison to AERONET measurements. *J. Atmos. Sci.*, **59**, 398–413.
- Veefkind, J. P., G. de Leeuw, P. A. Durkee, P. B. Russell, P. V. Hobbs,

- and J. M. Livingston, 1999: Aerosol optical depth retrieval using ATSR-2 and AVHRR data during TARFOX. *J. Geophys. Res.*, **104**, 2253–2260.
- Vermote, E., D. Tanré, J. Deuze, M. Herman, and J. Morcrette, 1997: Second simulation of the satellite signal in the solar spectrum, 6S: An overview. *IEEE Trans. Geosci. Remote Sens.*, **35**, 675–686.
- Wagner, R., S. Nemesure, and S. Schwartz, 1997: Aerosol optical depth: High space and time resolution retrieval and error budget from satellite radiometry. *J. Atmos. Oceanic Technol.*, **14**, 577–590.
- Wetzel, M. A., and L. L. Stowe, 1999: Satellite-observed patterns in stratus microphysics, aerosol optical thickness, and shortwave radiative forcing. *J. Geophys. Res.*, **104**, 31 287–31 299.